Very high cycle fatigue crack initiation mechanism according to a 3D model of persistent slip bands formation in α-ferrite

Chong Wang, Qingyuan Wang, Danièle Wagner, Zhiyong Huang, Claude Bathias

VHCF crack initiation mechanism according 3D Micron Abreast Pipes model of PSB on α-ferrite

Journal:	*Fatigue & Fracture of Engineering Materials & Structures*
Manuscript ID:	Draft
Manuscript Type:	VHCF6
Date Submitted by the Author:	n/a
Complete List of Authors:	WANG, Chong; Sichuan University, Mechanics and Engineering Science HUANG, Zhiyong; Sichuan University, School of Aeronautics and Astronautics Wang, Qingyuan (VHCF6); Sichuan University, ; WAGNER, Daniele; University Paris X, ; ENSAM, Bathias, Claude; University of Paris, LEEE/ITMA
Keywords:	Irreversible deformation, Fatigue crack initiation, Threshold of fatigue crack, Very high cycle fatigue, Micron Abreast Pipes model

VHCF crack initiation mechanism according 3D Micron Abreast Pipes model of PSB on α-ferrite

Chong WANG[1], Qingyuan WANG[1], Danièle WAGNER[3], Zhiyong HUANG[2]*, Claude BATHIAS[3]

[1] Sichuan University, Department of Mechanics and Engineering Science, Chengdu, 610065, China

[2]Sichuan University, School of Aeronautics and Astronautics, Chengdu, 610065, China

[3]University Paris Ouest Nanterre La Défense, LEME Laboratory, Ville d'avray, 92410, France

Abstract: Paris's law of fatigue crack propagation rate is well applied in the defect-tolerance fatigue approach. When carry out same approach on the very high cycle fatigue (VHCF), the understanding of mechanism about fatigue crack initiation is obviously important. In the present work here, the fatigue crack initiation loaded in the VHCF regime was investigated by a new approach which combines the fracture surface analysis and fatigue crack thermal dissipation. The experiments were carried out on a sheet specimen under a 20 KHz ultrasonic frequency with images registration thermal or optical. A Micron Abreast Pipes model is established to introduce the relation between the damage accumulation of irreversible deformation and the fatigue crack. It is found that the transition between initiation and short crack propagation corresponds to the intrinsic threshold of fatigue crack. It takes more than 99% of the gigacycle fatigue life to achieve this transition size.

Keywords: Irreversible deformation, Fatigue crack initiation, Threshold of fatigue crack, Very high cycle fatigue, Micron Abreast Pipes model.

1. Introduction

It is a common understanding that the crack initiated from surface defect leads to fatigue failure in crystalline materials under cyclic loading. In the case of smooth surface, the localized cyclic plastic strain result in the surface relief. In f.c.c materials (which are the most studied materials),when strain reached to cyclic stress-strain curve plateau, localized deformation changes to the Persistent Slip Bands (PSB) instead of dislocation veins in matrix in order to accommodate the high value of plastic deformation[1]. The formation of PSBs arranges depending on low index crystallographic planes or grain orientation in another means. Extrusions and intrusions (where the egress of PSB) were estimated to explain the preferential sites for the nucleation of microcracks[2]. PSBs in polycrystals have typical thickness around 1 μm. Larger dimension of PSBs is in the same range of grain size. In bcc materials, like Armco iron, the identification of PSB is matter of debate[3-9]. The reason lies in the very different temperature and strain rate dependent dislocation glide behavior in body centered cubic (b.c.c) metals, as compared to f.c.c metals.

Paris's law of fatigue crack propagation rate is well applied in the defect-tolerance fatigue approach. When carry out same approach on the very high cycle fatigue, the corresponding loading is much lower than conventional fatigue. Therefore, under very high cycle fatigue loading, the effective stress intensity factor for a microcrack propagates from an intrusion is significantly lower than the conventional one. For a basic point of view, it is of interest to understand the initiation of a fatigue crack in the VHCF regime in single phase metals without internal defects. Limited studies at different loading conditions have given references of fatigue features on iron. Dislocation arrangement after fatigue bending test at low frequency are investigated by Mcgrath and Bratina[10]. They find that the average dislocation density for particular stress amplitude reaches a constant value after showing a rapid increase in the early portion of the fatigue life. When Wood et al[11] compare the fatigue mechanisms in b.c.c. iron and f.c.c. metals at low frequency in alternating torsion, they noted that at amplitudes above the SN knee, slip markings appeared on a specimen after a few cycles. At amplitude below the knee they appeared after a million or so cycles. Wei and Baker found wall developed arrays of dislocation loops in iron specimen after only 10 cycles in push-pull fatigue [12].

However, fatigue deformation features of iron at very high cycle fatigue regime are limited. Current work intends to investigating the fatigue initiation and localized irreversibility of b.c.c. metals (α-Fe) at very high cycle fatigue regime. In order to study facility observation of localized deformation on surface, a new flat specimen was designed to be tested at 20 kHz up to 10^{10} cycles. Observations were performed on specimen surface during testing and fractographic after failure.

2. Experimental

A polycrystalline iron was selected as object of study. Its chemical composition as indicates in Table 1. The microstructure is ferrite with equiaxed grains. The ferrite grain size is included in 10 to 40 μm. No specifically orientation was observed by EBSD. Yield Stress is 240 MPa.

For the reason of surface real time observation by IR camera and optical microscope (OM), 1 mm flat specimen (Fig. 1) was used for carrying out fatigue tests. Specimen, special attachment and piezoelectric fatigue machine constituted the resonance system working at 20 kHz. Before testing, both sides surface of flat specimen were polished. One surface was electrolytic etched for optical observation. Another side was painted in black to have the surface emissivity close to 1. The cyclic

loading is tension-compression. The stress ratio is then R = -1. Temperature of testing is maintained below 100 °C.

During ultrasonic fatigue loading, theoretically, the specimen center has zero axial displacement. A small area on the surface which includes specimen center remains visible by microscope because the displacement maintained at very low level. Therefore a mobile optical microscope constructed for taking the online image. It has magnification 320X and recording image at frequency up to 1 Hz. With this mobile optical microscope, it is possible to observe general appearance when character deformation takes place in the specimen surface like enforced slip bands. A CEDIP Orion infrared camera was used to record the temperature evolution during at another side. The frequency of the IR camera was 50Hz and the aperture time was 100 μs. The typical online observation system is shown at Fig. 2.

3. Results and discussions

Fig. 3 shows the evolution of irreversible deformation on specimen surface by increasing number of cycles. It is found that, irreversible slip bands formed at the beginning stage of fatigue loading. This slip bands are multiplied or grown in the same grain due to following cycle loading. At neighbor area, new irreversible slip bands formed independently in another grain where no deformation appears at previous 1.6×10^7 cycles. Grain, either one already with slip band or one without slip band can has new slip band occurrence within following cycle loading. At the slip bands site, most of irreversible slip bands formed before 2.9×10^8 cycles. Only slightly evolution occurs by cyclic loading during fatigue life between 2.9×10^8 and 10^{10} cycles. It suggests that new irreversible deformation Δd (relates to localized plastic strain) per each loading cycle $\Delta d/N$ is decreasing with increasing number of cycle. $\Delta d/N$ closing to zero after 2.9×10^8 cycles in this case. In other words, crack initiation due to cumulating further new irreversible deformation after 2.9×10^8 cycles is scattered dispersed. That may be the reason why the S-N curve is normally significantly dispersed at regime beyond 10^9 cycles.

Detail observations of surface irreversible slip bands or PSB under Scanning Electron Microscope (SEM) are given in Fig. 4. PSB formed by fatigue is localized deformation as described in f.c.c material but formed less individual. At investigation site, PSBs are found in 5 grains, where other grains remain undeformed at all. PSB is significantly changing the roughness of the original surface. PSBs at different grains were mainly in two directions which have angle close to 90°. Even in same direction, the PSB have clear end at grain boundary. It suggests that PSB is anchored at grain

boundary. PSB could active slip system in neighbor grain by enforce the stress concentration at inter boundary, but not go across the grain boundary at crack initiation stage. EBSD analysis shows that, same slip band direction always in the similar oriented grain (see slip band in red grain and orange grain). When neighbored grains have big difference in crystalline orientation, direction of slip band in different grain were almost perpendicular to each other (see slip band in red grain and blue grain).

A specimen with pronounced PSBs was investigated by SEM in three perpendicular surfaces to understand PSB in steric. The three surfaces are: original specimen surface, axial cutting surface and cross cutting surface, as shown in Fig. 5a. All three surfaces were processed by carefully mechanical polish and 4% Nital etching.

On the cross section (Fig. 5b), it appears equiaxed hollows separated or not by a thin wall of matrix (in nanoscale). Hollows are distributed linear in several lines as marked in the yellow line. Those lines with hollows are parallel. Equiaxed hollow has size in 0.5 μm. Hollow lines observed here have length about 3 μm to 5 μm. The distance between hollow lines is approximate 2 μm. Characters were found similarly on the axial cutting surface and original surface, as shown in Fig. 5c. Longitudinal slots were found pronouncedly. Slots in each grain are parallel. Orientation changing of slot takes place at grain boundary in almost 90°. It is reasonable to relate those slots to formation of PSB on the original specimen surface. It is found that the slots are shallow. It seems these slots are like cylinders. The width of each individual slot is around 0.5 μm, the distance between parallel slots varied from 1 μm to 3 μm and the length of slot is between 2 μm to 10 μm. Regarding this hollow deformation on cross section (Fig. 5b) and longitudinal slots on axial sections (Fig. 5c), it may be constructed a 3D schematic figure of the slots and hollows as Micron Abreast Pipes in Fig.5d.

Relation between crack initiation and irreversible deformation has been investigated through observations by OM on the surface, SEM on fracture surface and TEM on cutting film of deformed grain. Initiation area would be identified combining thermal analysis on surface[14, 15] and visually of grain boundary on fractograpy. Surface observations of cracked specimen show as in Fig.6. White arrow indicates a grain which has PSBs in it. In this PSB grain, crack opens along the PSBs which formed long time before crack occurs in this grain. Yellow arrow indicates the crack along a grain boundary. Intergranular crack takes place at grain boundary between two grains whose PSB are perpendicular to each other. Blue arrows denoted a transgranular crack. Crack stairs in the surface of this grain correspond to the appearance of slip bands beneath the fracture surface.

Fracture surface gives more interesting results. Three types of pattern were found in the initiation area: one intergranular and two transgranulars. The intergranular pattern is seen in Fig.7a. This intergranular crack appears not smooth, but presents a very fine linear structure on the grain surface which believes related to the dislocation slips. Moreover, two lines of hollows separated by around 2 μm are visible. The first type of transgranular crack is shown in Fig. 7b. The fracture surface through the grain is developed as a staircase. The distance between two stairs is about 2 μm. It suggests the same mechanism that those forming the stair structure in the surface as blue arrows in Fig.6. The second pattern of transgranular crack is shown Fig.7c. In this transgranular case, the fracture surface is composed of longisectional pipes arranged side by side. The diameter of the pipes is 0.5 μm in average. It corresponds to PSB on the surface indicated by white arrows in Fig.6. Detail observation in nano scale shows the pipe-end like structure on the fracture surface, Fig. 7d. It has same size (0.5 μm) either with hollow in Fig. 7a or with pipes in Fig. 7c.

A thin film (100 nm) was taken by FIB through the cross section of a PSB from one grain. The TEM observation is shown in Fig. 8. The white color corresponds to the matrix and the black color corresponds to the volume, which has higher density of dislocation. A circle in diameter about 0.5 μm clearly found.

A mechanism approach of crack initiation was provided base on fracture surface pattern as PSB and Micron Abreast Pipes model seen in Fig.5. An illustration of this fracture mechanism is schematically reported on the Fig. 9. The staircase structure, Fig. 7b, is probably a fracture occurring partially on abreast pipes, and crossing over to abreast pipe just below or above. The distance between two stairs is about 2 μm, in good agreement with the distance between two abreast pipes. In the case of second transgranular pattern Fig.7c, the crack path is entirely through abreast pipes in the same slip plane. The characteristic dimension of this pattern is pipe diameter about 0.5 μm. The line of hallows (separated in distance about 2 μm) seen on the intergranular crack as in Fig. 7a and on the cross section as in Fig. 5b are probably the end of abreast pipes at grain boundary (in good agreement with the distance between two neighbored pipes). However, abreast pipes sometime may linked cross the nanoscale wall between pipes to form subscale 2 dimensions planar default as small facets denoted by yellow arrows in Fig 7b. The internal irreversible plastic deformations as the Micron Abreast Pipes model potentially facilitate the fatigue crack initiation.

According the discussion above, it can conclude here that very high cycle fatigue crack initiate not only by extrusion and intrusion, but also due to irreversible slip bands in the subsurface. It starts from the

irreversible slip bands in the surface, which induces stress concentration and produces the occurrence of PSB in subsurface[13]. The irreversible slip bands in the subsurface makes easier the fatigue crack initiation stage. Fatigue crack at subsurface at initiation stage is form by connecting subscale defaults, such as Micron Abreast Pipes in same slip plane, inharmonious of deformation at grain boundary or links between small facets of irreversible slip bands. Regarding fatigue propagation threshold and temperature elevation[14-16], it may estimate following mechanism of fatigue initiation in ferrite at VHCF regime. PSB occurs on specimen surface at beginning stage of VHCF test. With following loading cycles, more PSBs formed in surface and subsurface, evidently at location of initiation area. It means material volume in a small initiation area is damaged by PSB but not opened by a crack. PSBs and other multiplied dislocation lines make more volume at initiation area extended and weak to undertake the long range stress. Therefore pronouncedly stress concentration takes place in front of area extended. Consequently extended area grown to the edge of initiation area which correspond to the fatigue stress intensity factor threshold $\Delta K_{th}=E\sqrt{b}$ (Herzberg-Paris-McClintock law)[15,17]. By sufficient stress concentration, the initiation area opened suddenly and remained some area with character during initiation damaged. As blue arrows in Fig 7, between two slip planes, crack at stairs shows no plastic deformation on surface. The temperature recording[15] of VHCF test has shown that the crack initiation stage occurs at the end of VHCF test (less than 1% of the total life). Combining the evolution of irreversible deformation discussed above, it can conclude that more than 99% of the total life is takes up by the micro-damage due to forming PSBs in surface and subsurface, especially initiation area. The first fatigue crack appears on the specimen surface, the entire crack initiation zone appears supervening by connecting all defaults in the bulk material with in short time at end of VHCF.

4. Conclusions

1) Irreversible deformation (PSB) forms on the surface specimen at the beginning stage of VHCF.

2) Irreversible deformation can growth or multiplies independently with previous one. In VHCF regime (beyond 10^8 cycles) new irreversible deformation per each loading cycle $\Delta d/N$ is decreasing by increasing number of cycle.

3) Irreversible plastic deformations in bulk facilities the fatigue crack initiation. A Micron Abreast Pipes model in 3D provides to investigate the fatigue crack initiation mechanism.

Acknowledgements

This research was supported by the grant from the National Agency of Research, France (ANR) (DISFAT project, No. ANR-09-BLAN-0025-09). The authors also thanks the support from National

Science Research Foundation of China (No. 11372201 and No. 11327801) and the grant from Sichuan University (No. 2014SCU11063) .

References

[1] Suresh S (1998). Fatigue of materials (second edition). Cambridge university press, Cambridge, UK.

[2] Bathias C, Pineau A (2011). Fatigue of Materials and Structures: Application to Design. John Wiley & Sons, Hoboken, USA.

[3] Mughrabi H (1980). The Strength of Metals and Alloys, pp.1615-1639, Haasen P, Gerold V, Kostorz G (Ed.), Pergamon Press, Oxford, UK.

[4] Hong YS, Lu YH, Zheng ZM (1991). Orientation Preference and Fractal Character of Short Crack in a Weld Metal. J. Mater. Sci., 26, 1821-1826.

[5] Mughrabi H, Herz K , Stark X (1976). The effect of strain-rate on the cyclic deformation properties of α-iron single crystals. Acta Metall., 24, 659–666.

[6] Mughrabi H, Herz K , Stark X(1981). Cyclic deformation and fatigue behavior of α-iron mono- and polycrystals, Int. J. Fract., 17, 198–218.

[7] Mughrabi H., Ackermann F. , Herz K. , Persistent slip bands in fatigued face-centered and body-centered cubic metals, Fatigue Mech ASTM-STP, 675 (1979), pp. 67–105

[8] Klesnil M, and Lukas P (1972). Effect of stress cycle asymmetry on fatigue crack growth. Mater. Sci. Engng., 9, 231–40.

[9] Sommer C, Mughrabi H, Lochner D (1998). Influence of temperature and carbon content on the cyclic deformation and fatigue behavior of α-iron. Acta Mater., 46, 1527–1546.

[10] Mcgrath JT, Bratina W J (1965). Dislocation structures in fatigued iron-carbon alloys. Philos. Mag., 12, 1293-1305.

[11] Wood WA, Reimann WH, Sargant KR (1964). Comparison of Fatigue Mechanisms in Bcc Iron and Fcc Metals. Transactions of the Metallurgical Society of AIME, 230, 511-518.

[12] Wei RP, Baker AJ (1965). Observation of dislocation loop arrays in fatigued polycrystalline pure iron. Philos. Mag., 12, 1087-1091.

[13] Wang C, Wagner D, Wang QY, Bathias C (2012). Gigacycle fatigue initiation mechanism in

Armco iron. Int. J. Fatigue, 45, 91-97.

[14] Wang C, Blanche A, Wagner D, Chrysochoos A, Bathias C (2014). Dissipative and microstructural effects associated with fatigue crack initiation on an Armco iron. Int. J. Fatigue, 58, 152-157.

[15] Wang C, Wagner D, Bathias C (2014). Investigations on the fatigue crack propagation threshold in Very High Cycle Fatigue. Adv. Mater. Res., 891, 357-362.

[16] Ranc N, Wagner D, Paris PC (2008). Study of thermal effects associated with crack propagation during very high cycle fatigue tests Original Research Article. Acta. Mater., 56, 4012-4021.

[17] Bathias C, Paris PC (2010). Gigacycle fatigue of metallic aircraft components. Int. J. Fatigue, 32, 894-897.

Table 1: Chemical composition of studied material

C	P	Si	Mn	S	Cr	Ni	Mo	Cu	Sn	Fe
0.008	0.007	0.005	0.048	0.003	0.015	0.014	0.009	0.001	0.002	Balance

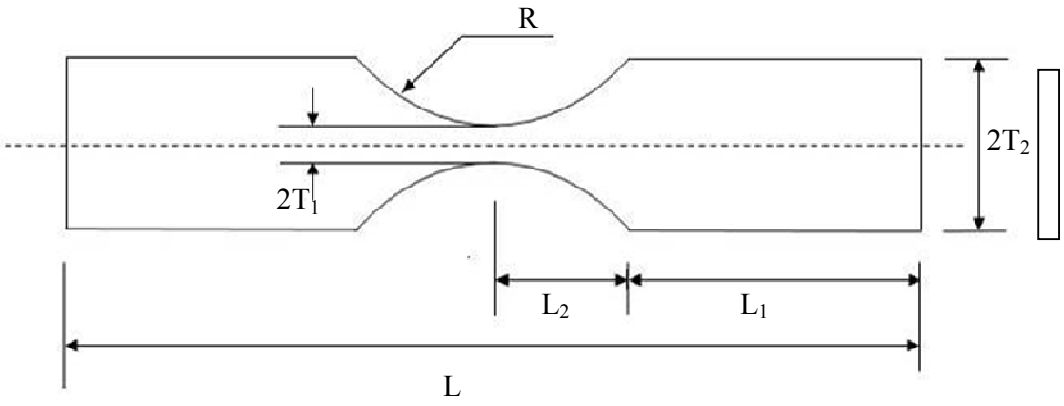

Fig 1. Sketch of flat ultrasonic specimen

Fig. 2 Experimental system

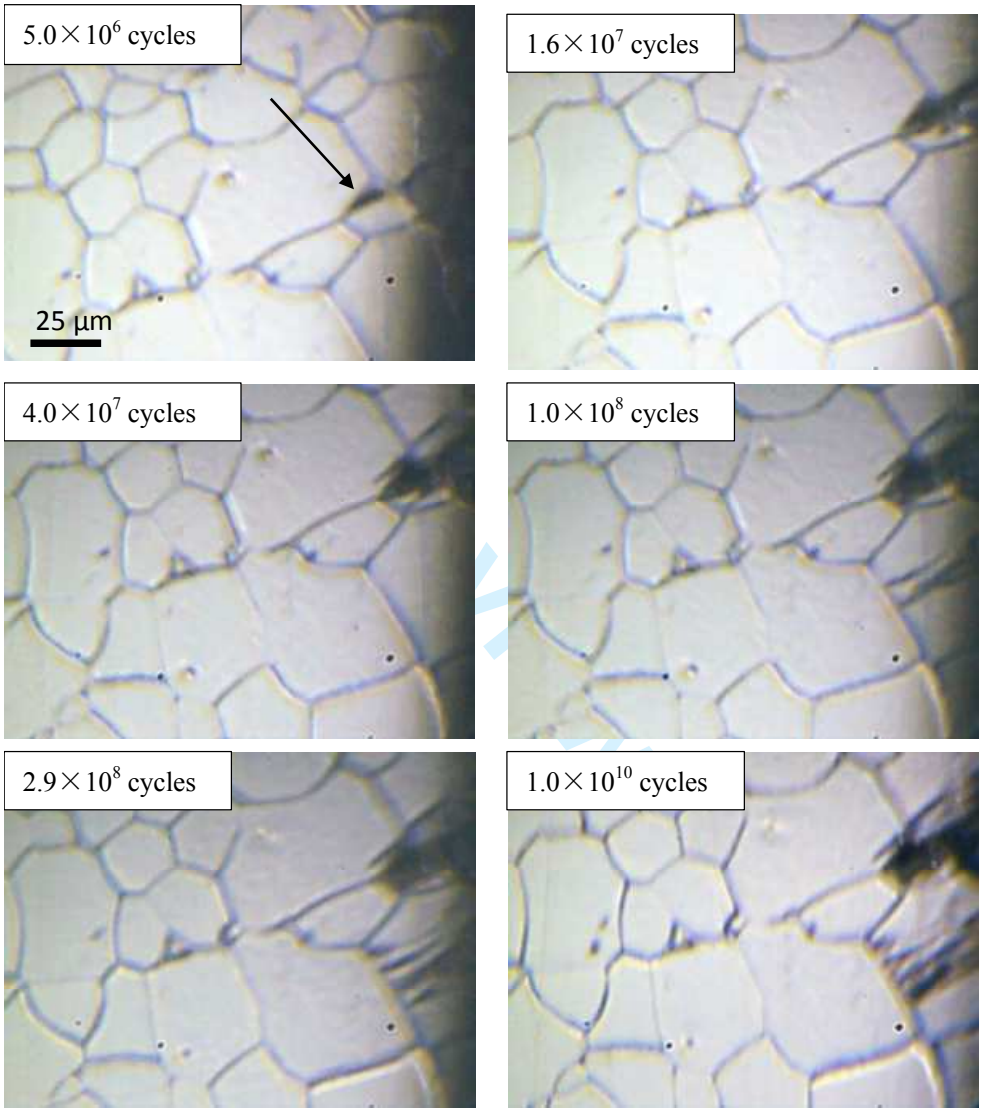

Fig. 3 Evolution of surface irreversible deformation

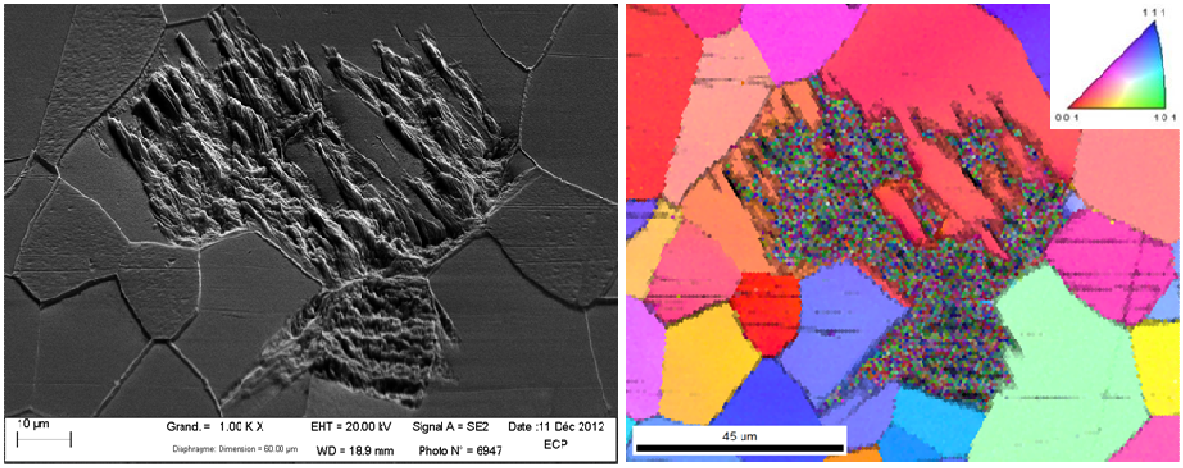

Fig. 4 PSB surface observation by SEM and EBSD analysis

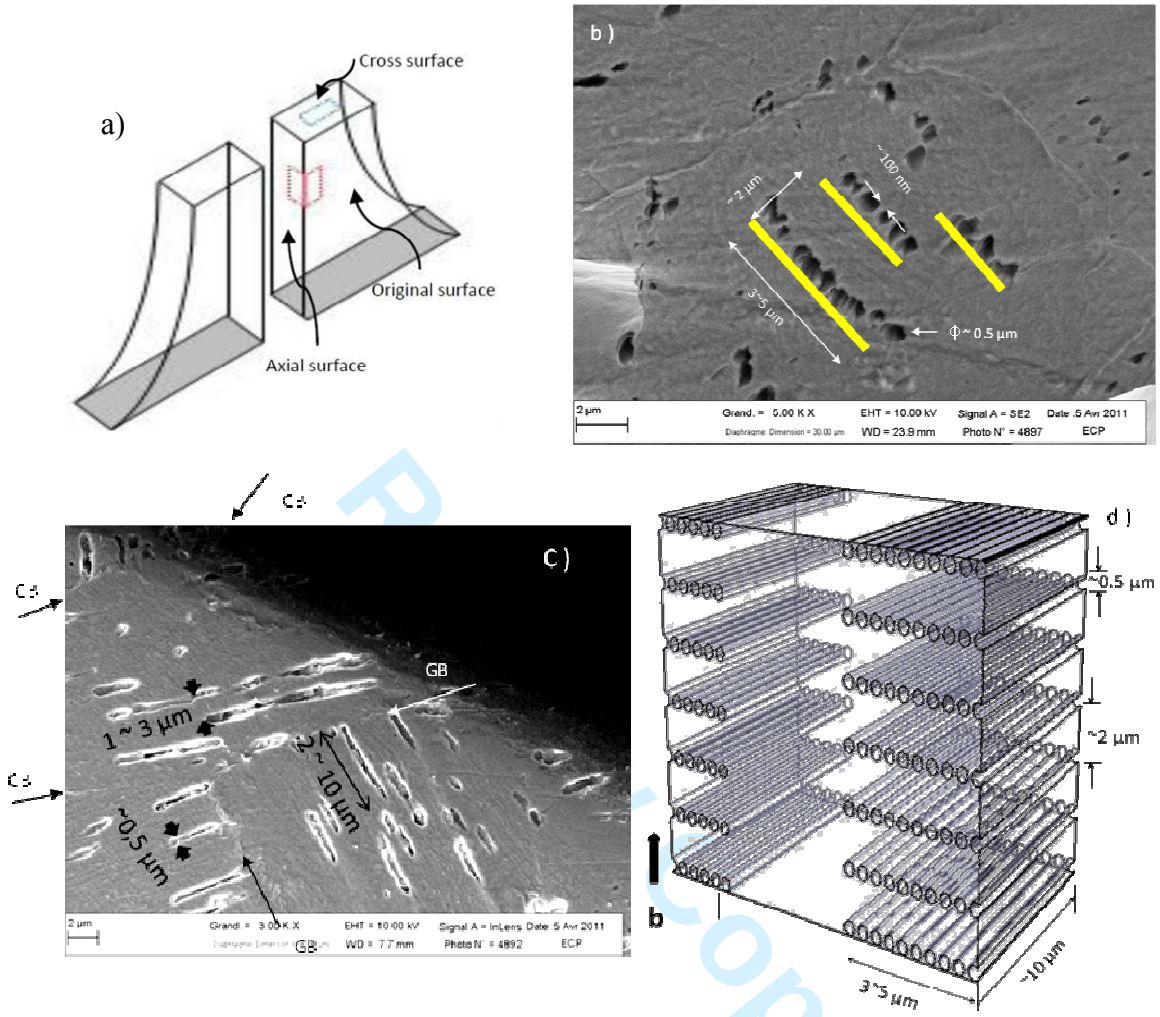

Fig. 5 The Structure of PSB in three sections after polish and the illustration of PSB by Micron Abreast Pipes model

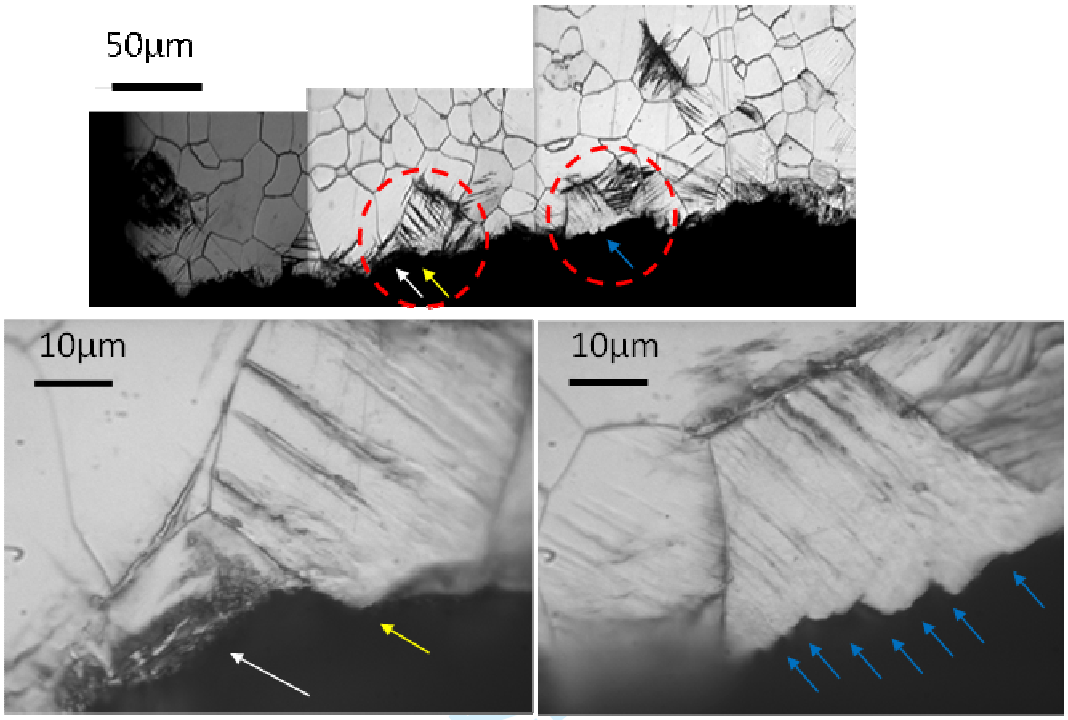

Fig. 6 Surface observation at crack initiation area of a cracked specimen

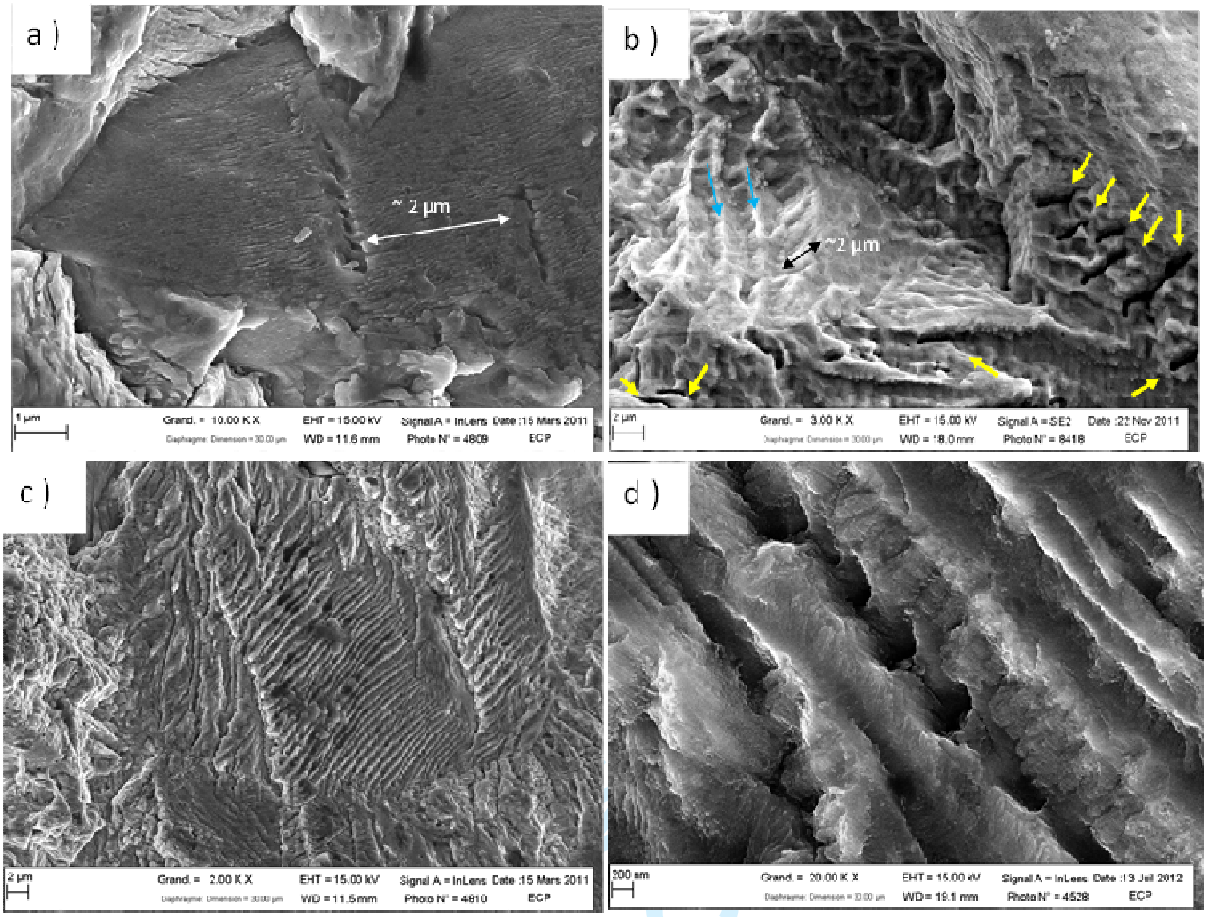

Fig.7 Pattern characters on crack surface at initiation area

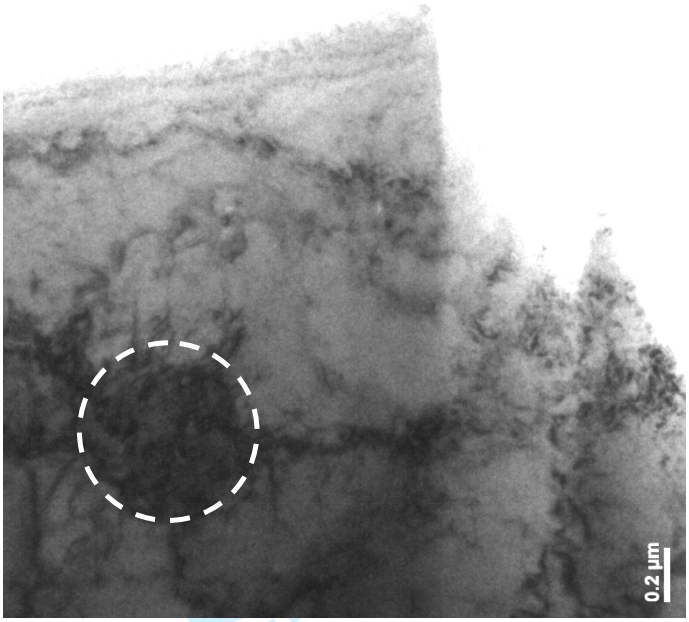

Fig. 8. TEM observation of a FIB film from the cross section of a PSB at initiation area

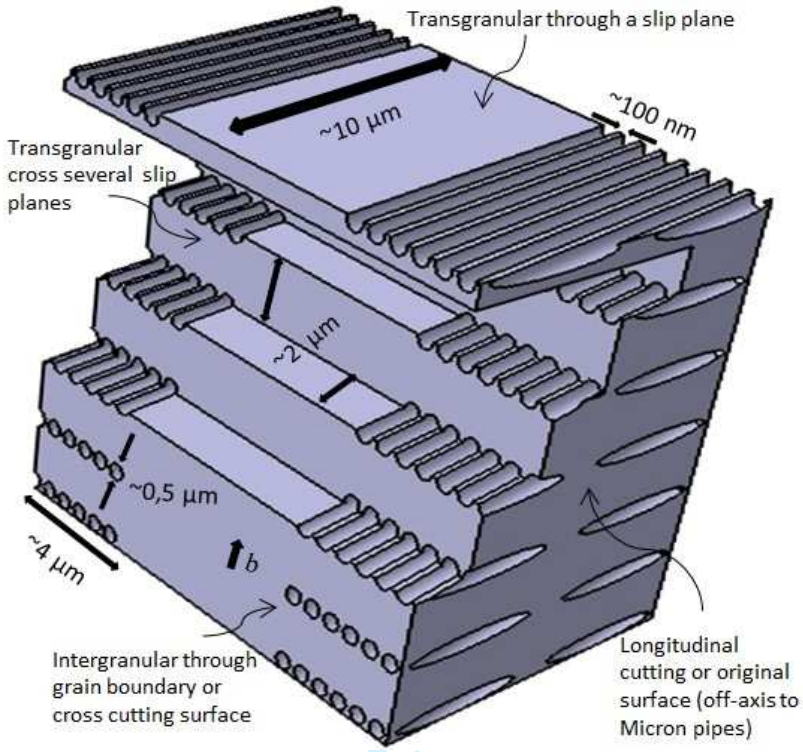

Fig. 9.Illustration of crack initiation mechanism by 3D Micron Abreast Pipes model of PSB